Mutational Analysis of Posttranslational Heterocycle Biosynthesis in the Gyrase Inhibitor Microcin B17: Distance Dependence from Propeptide and Tolerance for Substitution in a GSCG Cyclizable Sequence†

Ranabir Sinha Roy, Peter J. Belshaw, and Christopher T. Walsh*

Department of Biological Chemistry and Molecular Pharmacology, Harvard Medical School, Boston, Massachusetts 02115

Received November 18, 1997

ABSTRACT: Microcin B17 (MccB17) is a peptidyl antibiotic that is secreted in stationary phase by several strains of *Escherichia coli.* The antibiotic efficacy of this polypeptide depends on the posttranslational modification of eight cysteine and serine residues to thiazoles and oxazoles, respectively, within the 69 aa McbA structural gene product. Mono- and bisheterocycle formation is mediated by MccB17 synthetase, an enzyme complex composed of three proteins: McbB, -C, and -D. After substrate processing, an N-terminal 26 aa propeptide sequence is cleaved to afford the mature antibiotic. A method for the overexpression and rapid purification of microcin synthetase has been developed using a calmodulin-binding peptide tag. The determinants of substrate recognition and synthetase-mediated heterocycle formation were investigated by a systematic evaluation of 15 $McbA_{1-46}$ analogues representing minimal substrates containing the first bisheterocyclization site (Gly^{39}-Ser^{40}-Cys^{41}-Gly^{42}) and variants thereof. Each substrate analogue was overexpressed and affinity-purified as fusions to maltose-binding protein, incubated with purified synthetase, and evaluated for processing by Western blots, UV spectroscopy, and mass spectrometry. Insights gained into the process of enzymatic heterocycle formation from cysteine and serine residues are discussed, including the distance dependence of the first cyclized residue from the propeptide and the local sequence context at the cyclizable sites. A model for McbA substrate recognition and processing by MccB17 synthetase is proposed.

While *Escherichia coli* are generally not regarded as antibiotic producers, certain strains synthesize low molecular weight antibacterial compounds known as microcins (*1*). The microcin B17 operon with seven genes (*mcbA*−*G*, Figure 1A) (*2*, *3*) is a well-characterized example and is of interest both for the enzymatic posttranslational modifications and for the mode of action of the 3.1 kDa peptidyl antibiotic. Mature microcin B17 with antibacterial activity arises from a prepro-form (Figure 1B), which is a 69 residue polypeptide product of the *mcbA* gene (*4*, *5*). As illustrated in Figure 1B, McbA (prepromicrocin B17) is subjected to an iterated series of posttranslational cyclizations, dehydrations, and aromatizations mediated by the gene products of *mcbBCD*, which convert 14 of the 69 residues into 8 heterocycles (4 oxazoles and 4 thiazoles) to generate promicrocin B17 (*6*−*8*). Subsequent proteolytic removal of the first 26 residues (the propeptide) yields mature microcin B17, which is exported out of the producing cell by an ABC type cassette system encoded by *mcbE* and *mcbF* (*9*). The mono and 4,2-fused bisheterocycles in MccB17[1] probably target it for intercalation into DNA in a complex with DNA gyrase, its proposed target of antibiotic action (*10*). DNA gyrase is an important target for antibacterial therapy since it is the site of action of the quinolone class of anti-infective drugs (*11*).

Structure−function studies of McbA are of interest to understand which of the planar heterocycles are essential for DNA gyrase inhibition, and to gain insight into the minimal structure and sequence requirements for antibacterial activity. To this end, it would be useful to evaluate the chemoselectivity and regiospecificity of the posttranslational machinery that converts Gly-Ser, Gly-Cys, Gly-Ser-Cys, and Gly-Cys-Ser peptidyl moieties in the McbA substrate to the oxazole, thiazole, and 4,2-fused oxazole−thiazole and thiazole−oxazole groups, respectively. We have recently established posttranslational roles for McbB, -C, and -D, as subunits in a purified microcin synthetase complex that converts prepromicrocin B17 to promicrocin B17 (*12*). Notably, the activity of microcin synthetase requires ATP cleavage. Furthermore, substrate turnover demands the covalent attachment of the 26 aa propeptide ($McbA_{1-26}$) to the

† This research was supported by NIH Grant GM 20011 to C.T.W. R.S.R. is a Parke-Davis Fellow of the Life Sciences Research Foundation. P.J.B. is a Fellow of the Jane Coffin Childs Memorial Fund for Medical Research. This investigation has been aided by a Grant from the Jane Coffin Childs Memorial Fund for Medical Research.

* Corresponding author. Phone: 617-432-1715. Fax: 617-432-0556. E-mail: walsh@walsh.med.harvard.edu.

[1] Abbreviations: aa, amino acid(s); CBP, calmodulin-binding peptide; CIAP, calf intestinal alkaline phosphatase; dNTP, deoxynucleotide triphosphate; DTT, DL-dithiothreitol; EDTA, ethylenediaminetetraacetic acid (disodium salt); EGTA, ethylene glycol bis(*β*-aminoethyl ether)-*N*,*N*,*N*′,*N*′-tetraacetic acid; *γ*-CRS, *γ*-carboxylation recognition site; HPLC, high performance reversed-phase liquid chromatography; HRP, horseradish peroxidase; IPTG, isopropyl 1-thio-*β*-D-galactopyranoside; MALDI-MS, matrix-assisted laser desorption ionization mass spectrometry; Mcc, microcin; LB, Luria−Bertani medium; MBP, maltose-binding protein; PCR, polymerase chain reaction; PMSF, phenylmethanesulfonyl fluoride; Tris·HCl, tris(hydroxymethyl)aminomethane hydrochloride; USE, unique site elimination; UV, ultraviolet; wt, wild type.

S0006-2960(97)02825-0 CCC: $15.00
Published on Web 03/05/1998

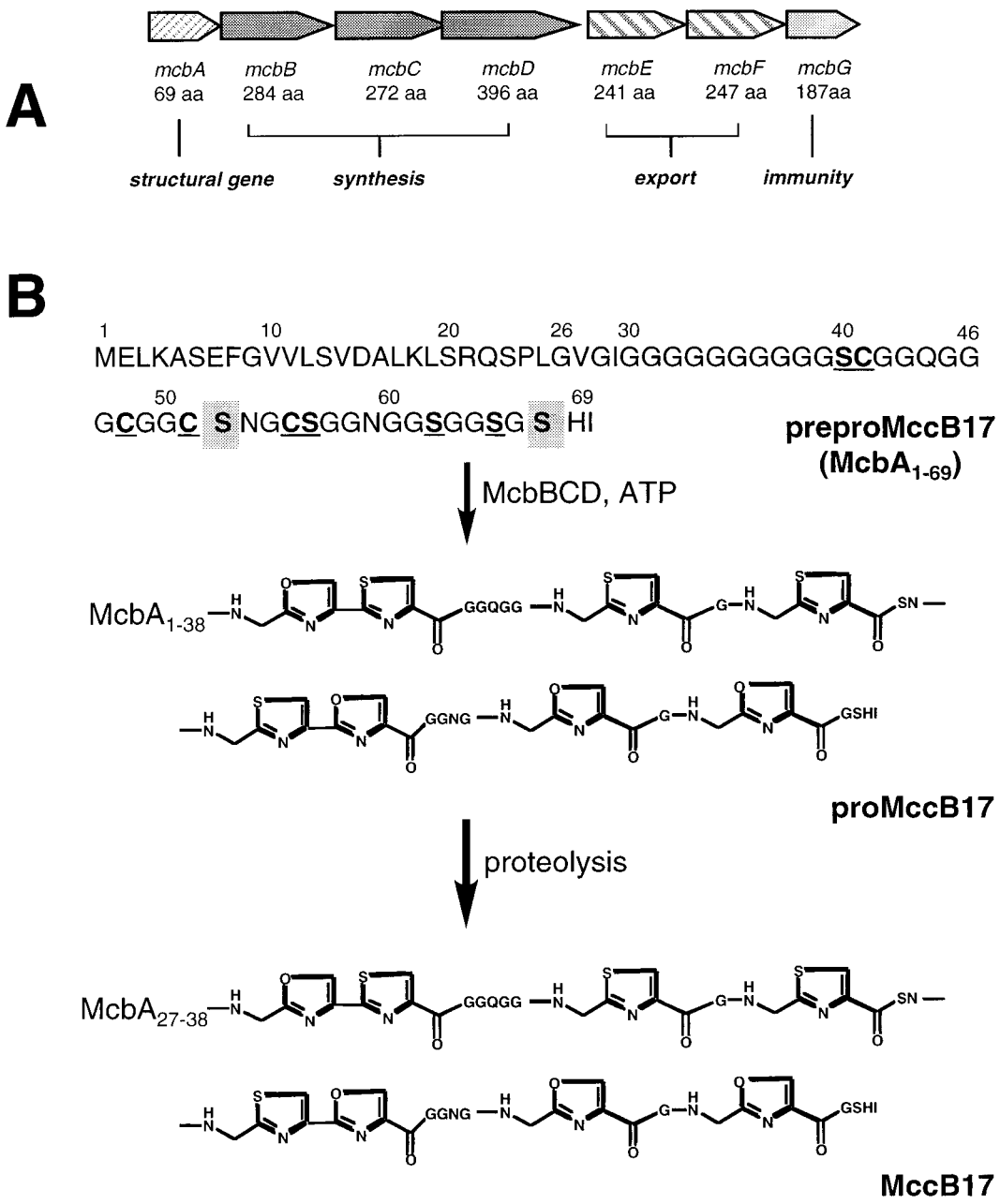

FIGURE 1: (A) Schematic of the seven genes *mcbA*−*G* constituting the microcin B17 operon. The functional roles of the gene products are depicted. (B) Maturation pathway of microcin B17. The polypeptide antibiotic is derived from a 69 aa precursor (preproMccB17), which is processed by MccB17 synthetase to afford proMccB17 incorporating eight heterocycles. Cyclized serines and cysteines are underlined and in boldface. Unprocessed serines are shaded. The N-terminal propeptide ($McbA_{1-26}$) is subsequently cleaved by an unidentified protease to afford mature antibiotic.

downstream polypeptide that is to be modified (*12*, *13*). Thus, the 46 residue fragment $McbA_{1-46}$ is a substrate for conversion of Gly^{39}-Ser^{40}-Cys^{41} to the bisheterocycle, whereas neither $McbA_{27-46}$ nor $McbA_{27-69}$ functions as a substrate or an inhibitor. In addition, since $McbA_{1-26}$ itself is a potent inhibitor, it appears that the McbBCD microcin synthetase has most or all of its initial recognition directed toward the propeptide region before the processing of downstream cyclizable Ser and Cys residues.

Herein, we have focused on $McbA_{1-46}$ as the minimal substrate for microcin synthetase to begin deconvoluting the recognition determinants in this system. The distance dependence between propeptide and the first residue cyclized (Ser^{40}) and the tolerance for residues other than glycine immediately upstream and downstream of Ser-Cys (native sequence -Gly^{39}-Ser^{40}-Cys^{41}-Gly^{42}-) have been assessed. We report results from a combination of mutagenesis in the $McbA_{1-46}$ framework, purification of MBP−$McbA_{1-46}$ fusion proteins, kinetic assays of microcin B17 synthetase using Western blots, and confirmation of heterocycle content in peptide products by UV and mass spectroscopies.

EXPERIMENTAL PROCEDURES

Materials. Bacteriological media were obtained from Difco Laboratories. Competent *E. coli* strain BL21(DE3) and restriction-grade thrombin were purchased from Novagen. Competent *E. coli* strain DH5α was purchased from GibcoBRL. Competent *E. coli* strain XL*mutS* Kan^s for site-directed mutagenesis, plasmid pCaln, calmodulin resin, and *Pfu* DNA polymerase were purchased from Stratagene.

Table 1: Oligonucleotide Primers for Site-Directed Mutagenesis[a]

No.	Function	5′→3′ Nucleotide Sequence
1	$McbA_{1-46}$ *Bam*HI	AGGAG**GATCC**ATGGAATTAAAAGCGAGTGAATTTG
2	$McbA_{1-46}$ *Msc*I, *Hin*dIII	CCAC**A**A**GCTTA**GCCACCTTG**G**CCACCGCAGCTAC
3	USE, *Sma*I removal	CTGGAATGCTGTTTT**A**CC**A**GG**T**ATCGCAGTGGTG
4	$McbA_{1-46}$ *Avr*II	CGCCAGTCTCC**CC**TAGGTGTTGGCAT
5	$McbA_{1-46}$ polyGly (+ strand)	CTAGGTGTTGGCATTGGTGGTGGTGGCGGTGGAGGTGGTGGAGGTAGCTGC GGTGG
6	$McbA_{1-46}$ polyGly (- strand)	CCACCGCAGCTACCTCCACCACCTCCACCGCCACCACCACCAATGCCAA CAC
7	USE, *Cla*I removal	CCCATACAATCG**G**TAGATTGTCGCAC
8	GSTG	TGGTGGAGGTAGC**AC**CGGTGGCCAAGG
9	GTCG	GGAGGTGGTGGAGGTA**C**CTGCGGTGGCCAAGG
10	GSCN	AGGTAGCTGC**AA**TGGCCAAGG
11	ASCG	GGAGGTGGTGGAG**C**TAGCTGCGGTGGCCAAGG
12	DSCG	GGAGGTGGTGGAG**AC**AGCTGCGGTGGCCAAGG
13	KSCG	GGAGGTGGTGGA**AAA**AGCTGCGGTGGCCAAGG
14	GSCA	AGGTAGCTGCG**C**TGGCCAAGG
15	GSCH	GGTGGAGGTAGCTGC**CA**TGGCCAAGGTGGCTAAGCTTGC
16	GSCD	AGGTAGCTGCG**A**TGGCCAAGG
17	GSCV	AGGTAGCTGCG**T**TGGCCAAGGTGG
18	PCR *Hin*dIII	CGTGAACCATCACCCTAATCAAG
19	$G_{11}SC$	**GA**TC**C**CT**AGGT**GT**T**G**GCATTGG**TGGTGGTGGTGGCGGTGGAGGTGGTGGAG GTAGC
20	G_9SC	**GATCCCTA**G**G**TG**TTGGCATT**GGTGGTGGCGGTGGAGGTGGTGGAGGTAGC
21	G_7SC	G**ATCCCTAGG**TG**T**TGG**CAT**TGGCGGTGGAGGTGGTGGAGGTAGCTGC
22	G_5SC	GCAT**CCTA**GGTG**T**TGGC**AT**TGGAGGTGGTGGAGGTAGCTGC
23	G_3SC	GGTGG**CCTA**GG**T**G**T**TGG**CAT**TGGTGGAGGTAGCTGCGGTGGCCAAGG
24	$McbB_{BamHI}$	G**A**T**CGATCGG**A**T**CC**ATGATCAATATTCTGCCGTTTGAG
25	$McbB_{AvaI}$	CACCATCACATTTCCATTGTTCCCGGG

[a] Mismatch bases are underlined and in boldface.

Restriction endonucleases, T4 DNA ligase, T4 polynucleotide kinase, T4 DNA polymerase, calf intestinal alkaline phosphatase (CIAP), and amylose resin were obtained from New England Biolabs. Low molecular weight markers for polyacrylamide gel electrophoresis were obtained from Bio-Rad. HRP-conjugated goat anti-rabbit IgG (H+L) polyclonal antibody was purchased from Pierce. Polyclonal rabbit anti-MccB17 antibodies were generated by East Acres Biologicals. Plasmid pIADL14 encoding MBP−VanX fusion protein and plasmid pPY113 encoding the microcin B17 operon have been described previously (*5*, *14*).

Recombinant DNA Methods. Recombinant DNA techniques were performed as described elsewhere (*15*). Preparation of plasmid DNA, gel purification of DNA fragments, and purification of polymerase chain reaction (PCR) amplified DNA fragments (*16*) were performed using a QIAprep spin plasmid kit, a QIAEX II gel extraction kit, and a QIAquick PCR purification kit, respectively (QIAGEN). Oligonucleotide primers were obtained from Integrated DNA Technologies or Gene Link. PCR experiments were performed in 100 μL reaction mixtures containing 1× cloned *Pfu* polymerase reaction buffer (Stratagene), 200 μM each dNTP, 1 μM each PCR primer, approximately 100 ng of template, 10% DMSO, and cloned *Pfu* polymerase (2.5 units). The fidelity of DNA fragments was established by nucleotide sequencing after subcloning into the expression vector.

Construction of the Expression Vector for MBP−$McbA_{1-46}$. The expression vector for MBP−$McbA_{1-46}$ was constructed from plasmid pIADL14, a pET28b(+) derivative that encodes for maltose-binding protein (*17*) fused downstream to the *VanX* gene from type A vancomycin-resistant *Enterococci* (*14*).

$McbA_{1-46}$ was PCR-amplified from plasmid pPY113 (*5*) with primers 1 and 2 (Table 1), which introduced a *Bam*HI site at the 5′ terminus, a stop codon and a *Hin*dIII site at the 3′ terminus, and a silent *Msc*I site 14 bases upstream of the latter. The purified DNA fragment was digested with *Bam*HI and *Hin*dIII and subcloned into plasmid pIADL14 to afford plasmid pMSS1 (*M*icrocin *S*ynthetase *S*ubstrate). A silent *Avr*II site was introduced at the 3′ end of the $McbA_{1-46}$ propeptide coding sequence by Unique Site Elimination (USE) mutagenesis (*18*) of the single *Sma*I site in the vector (primers 3 and 4) to produce plasmid pMSS7. Next, the

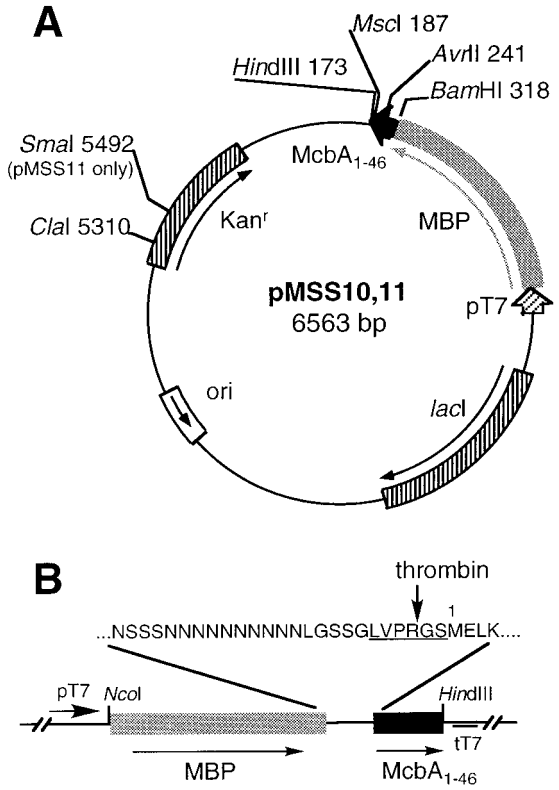

FIGURE 2: Vectors pMSS10 and pMSS11 constructed for the expression of MBP−$McbA_{1-46}$ fusion proteins. Kan^r, kanamycin resistance; *lac*I, *lac*I repressor; MBP, maltose-binding protein; ori, origin of ColE1 plasmid replication; pT7, T7 promoter; tT7, T7 terminator; $McbA_{1-46}$, $McbA_{1-46}$ gene. (B) Details of the MBP−$McbA_{1-46}$ fusion junction depicting the serine/asparagine-rich linker and the thrombin recognition site (underlined residues). Thrombin proteolysis occurs between Arg^{-3} and Gly^{-2} to afford $McbA_{1-46}$ with an N-terminal Gly-Ser dipeptide preceding Met^1 of the wild-type $McbA_{1-46}$ sequence.

polyglycine coding sequence in $McbA_{1-46}$ was rewritten with reduced codon degeneracy to minimize incorrect priming during PCR and site-directed mutagenesis. Two independent strategies were adopted toward this end. The complementary synthetic oligonucleotides 5 and 6, which code for the rewritten *Avr*II−*Msc*I fragment in $McbA_{1-46}$, were 5′-phosphorylated, annealed, and ligated into the pMSS7 backbone (digested with *Avr*II and *Msc*I and dephosphorylated with CIAP). The resulting plasmid pMSS10 encodes for $McbA_{1-46}$ fused in-frame with and downstream of maltose-binding protein (MBP, Figure 2A). A similar plasmid (pMSS11) was obtained by PCR mutagenesis of pMSS7 with primers 1 and 6, and subcloning the PCR product into pMSS1 using the *Bam*HI and *Msc*I sites. Plasmids pMSS10 and pMSS11 are identical except for retention of the unique *Sma*I site in the latter. Both expression vectors were used as template plasmids in subsequent PCR/USE-based site-directed mutagenesis. The asparagine-rich linker in the MBP−$McbA_{1-46}$ fusion protein incorporates a thrombin restriction site (LVPRGS), which upon proteolysis leaves the N-terminal dipeptide sequence Gly-Ser at positions −2 to −1 relative to the starting Met residue of $McbA_{1-46}$ (Figure 2B).

Site-Directed Mutagenesis. All site-directed mutants were constructed by USE mutagenesis of plasmids pMSS10 or pMSS11 except for the constructs listed in the next section. Selection primers 3 and 7 incorporate silent mutations that eliminate the *Sma*I and *Cla*I sites in these template plasmids, respectively. The appropriate selection primer was used in combination with mutagenic primers 8−17, which introduce specific mutations in the $McbA_{1-46}$ gene (*18*). Introduction of the desired mutation was confirmed by oligonucleotide sequencing with vector primers.

The polyglycine linker mutants G_nSC ($n = 11, 9, 7, 5, 3$) were constructed by PCR mutagenesis of plasmid pMSS10 with the sense/antisense primer pairs 19/18, 20/18, 21/18, 22/18, and 23/18, respectively, and subcloned back into pMSS10 using the *Avr*II and *Hin*dIII sites.

Overexpression of the MBP−$McbA_{1-46}$ Fusion Proteins. Cultures were grown in LB medium at 37 °C supplemented with kanamycin (50 μg/mL). One colony of freshly transformed *E. coli* strain BL21(DE3) was grown overnight at 37 °C in 5 mL of medium, and 2.5 mL of this culture was used to inoculate 250 mL of LB-kanamycin. The inoculum was grown at 37 °C to an OD_{600} of 0.6, and IPTG was added to a final concentration of 1 mM. Cells were harvested 3.5 h later by centrifugation and used immediately.

Purification of MBP−$McbA_{1-46}$ Fusion Proteins. All steps were performed at 4 °C unless otherwise noted. Cell pellets from 250 mL of culture were resuspended in 20 mL of buffer A (20 mM Tris·HCl, pH 7.5, 200 mM NaCl, 1 mM EDTA, 1 mM DTT), containing chymostatin (1 μg/mL), leupeptin (1 μg/mL), aprotinin (2 μg/mL), and PMSF (200 μM), and disrupted twice in a French pressure cell (18 000 psi). Cellular debris was removed by centrifugation (95000*g*, 30 min), and the supernatant was applied to an amylose column (10 × 60 mm, 0.5 mL/min) previously equilibrated with buffer A. The column was washed with 75 mL of buffer A (1 mL/min), and the desired MBP−$McbA_{1-46}$ fusion protein was eluted with buffer A containing 10 mM maltose. Fractions (1.8 mL each) containing the recombinant MBP−$McbA_{1-46}$ fusion protein were analyzed for purity by SDS−PAGE, pooled, and concentrated to 15−50 mg/mL with a Centriprep-30 concentrator (Amicon). Protein concentration was determined by UV−Vis spectroscopy, and extinction coefficients ($\epsilon_{280} = 66\,350\ M^{-1}\cdot cm^{-1}$ for all fusion proteins) were calculated based on a modification of the Edelhoch method (*19*, *20*). The concentrated protein samples were dialyzed for two changes against buffer B (50 mM Tris·HCl, pH 7.5). Alternatively, buffer exchange was accomplished using Centripep-30 concentrators. Protein samples were stored at −20 °C.

Construction of the Expression Vector for CBP-Tagged Microcin B17 Synthetase. Plasmid pCaln, a pET11a derivative, encodes calmodulin-binding peptide (*21*, *22*) under control of the T7 promoter and incorporates a downstream multiple cloning site (MCS) (*23*). This plasmid was used as the expression vector for the contiguous *mcbB*, *-C*, and *-D* genes in the microcin B17 operon. PCR amplification of plasmid pPY113 with the sense/antisense primer pair 24/25 afforded a 339 bp McbB gene fragment up to the internal *Ava*I site, with a *Bam*HI adapter site at the 5′-terminus. The purified PCR-amplified product was digested with *Bam*HI and *Ava*I, and, together with the 2.8 kb DNA fragment obtained by digestion of pPY113 with *Ava*I and *Sal*I (constituting the rest of *mcbBCD*), was subcloned into the pCaln backbone using the *Bam*HI and *Sal*I sites. The resulting plasmid pCalBCDn (Figure 3A) encodes *mcbBCD*, fused downstream of and in-frame with CBP (CBP−

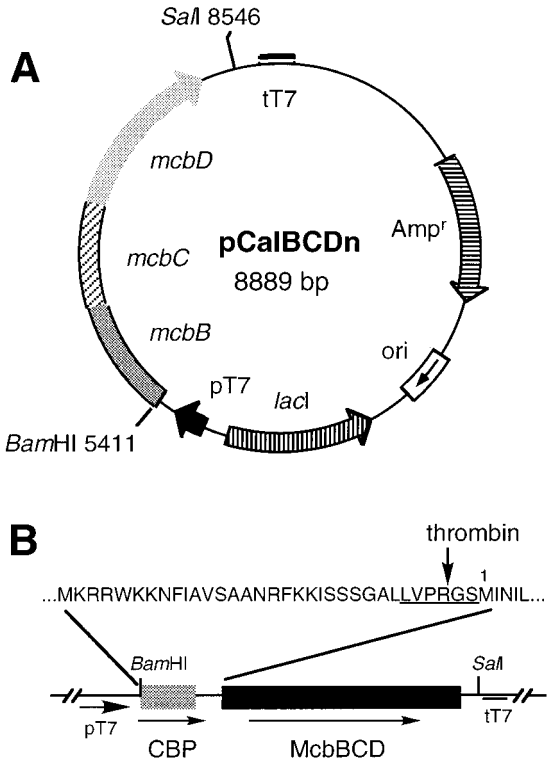

FIGURE 3: Vector pCalBCDn constructed for expression of CBP-tagged MccB17 synthetase. Amp^r, ampicillin resistance; *lac*I, *lac*I repressor; ori, origin of ColE1 plasmid replication; pT7, T7 promoter; tT7, T7 terminator; *mcbBCD*, genes encoding McbB, -C, and -D subunits of the synthetase, respectively. (B) Details of the MBP−McbA$_{1-46}$ fusion junction depicting the calmodulin-binding peptide (CBP). A thrombin recognition site is also present (underlined residues), although thrombin proteolysis was not performed. The N-terminus of the McbB subunit in this construct is tagged with CBP.

McbBCD). The *mcbB* gene product in this construct is tagged at the N-terminus with the 26 residue CBP polypeptide (Figure 3B).

Overexpression and Purification of CBP−BCD Synthetase. Cultures were grown in LB medium at 37 °C supplemented with ampicillin (150 μg/mL). Freshly transformed *E. coli* strain BL21(DE3) was grown overnight at 37 °C in LB/ampicillin, and 10 mL aliquots were used to inoculate 6 × 1 L of LB/ampicillin. The inoculum was grown at 37 °C to an OD$_{600}$ of 0.6, and IPTG was added to a final concentration of 400 μM. Cells were harvested 3 h later by centrifugation. All subsequent steps were performed at 4 °C unless otherwise noted. Cell pellets from the 6 L culture were resuspended in buffer C (50 mM Tris·HCl, pH 7.5, 150 mM NaCl, 1 mM DTT, 2 mM $CaCl_2$, 1 mM magnesium acetate), containing chymostatin (1 μg/mL), leupeptin (1 μg/mL), aprotinin (2 μg/mL), PMSF (100 μM), and 1 mM imidazole, and stored overnight at −80 °C. The thawed cells were disrupted twice in a French pressure cell (18 000 psi). Cellular debris was removed by centrifugation (95000g, 1 h), and the supernatant was applied to a calmodulin column (10 × 10 mm, 0.5 mL/min) previously equilibrated with buffer C. The column was washed with buffer C containing 1 mM imidazole and buffer C alone (20 mL each, 1 mL/min). Moderately pure CBP−McbBCD (elution 1) was eluted from the column with 34 mL of buffer D (50 mM Tris·HCl, pH 7.5, 150 mM NaCl, 1 mM DTT, 2 mM EGTA). Fractions (1.8 mL each) containing the recombinant CBP−McbBCD synthetase were analyzed for purity by SDS−PAGE, pooled, and concentrated to ∼0.5 mg/mL with an Ultrafree-15 concentrator (30 kDa cutoff, Millipore). Protein concentration was determined with Bradford reagent (Bio-Rad), using BSA as the standard. Synthetase of increased purity was subsequently eluted from the column (elution 2) with 65 mL of buffer E (50 mM Tris·HCl, pH 7.5, 300 mM NaCl, 1 mM DTT, 2 mM EGTA, 0.1% Triton-X100). Fractions (1.8 mL each) containing the pure CBP−McbBCD synthetase complex were analyzed for purity by SDS−PAGE, pooled, aliquoted, and stored at −80 °C. The yield of pure synthetase obtained from 6 L of induced *E. coli* BL21(DE3) cells was ∼6 mg.

Western Blot Assay for Synthetase Activity. Reaction mixtures consisted of 10−20 μM MBP−McbA$_{1-46}$ fusion protein, 50 mM Tris·HCl, pH 7.5, 125 mM NaCl, 20 mM $MgCl_2$, 2 mM ATP, 10 mM DTT, and purified CBP−McbBCD synthetase (∼ 0.06 mg/mL) in a volume of 60 μL. Synthetase of the same specific activity was used in assays that compared the kinetics of different McbA$_{1-46}$ mutants. Reaction mixtures were incubated at 37 °C, and 2 μL aliquots withdrawn at appropriate time points were electrophoresed on a 10% SDS−PAGE gel. The gels were transblotted to Immobilon-P PVDF membranes (Millipore) at 60 V for 70 min and subsequently analyzed by protein immunoblot (*24*) with rabbit polyclonal anti-MccB17 and goat anti-rabbit HRP-conjugated antibodies. Signal detection was accomplished using chemiluminescent SuperSignal substrate (Pierce) with exposure to Reflection NEF film (Dupont). Immunoblots were incubated with 1:5 dilutions of substrate in water for 3 min to avoid signal saturation. Developed films (15 s exposures) were scanned and quantified using NIH image version 1.61 software (NIH). Aliquots from a 30 min incubation of MBP−McbA$_{1-46}$ ("wild type") with synthetase were used as internal standards (duplicate lanes per gel) when comparing signals from multiple immunoblots. Alternatively, synthetase obtained in the first elution from the affinity chromatography purification was used in the Western assays. In these blots, nonspecific and consistent recognition of an ∼67 kDa contaminant in the synthetase preparation by the polyclonal rabbit antibody served as a convenient internal standard for each lane in the immunoblot. In each case, data were normalized to the appropriate standards used, and the standard deviation (σ_{n-1}) was typically less than 12% of the mean.

HPLC and Mass Spectrometry Analyses of Synthetase Activity. Reaction mixtures consisted of 20−140 μM MBP−McbA$_{1-46}$ fusion protein, 50 mM Tris·HCl, pH 7.5, 125 mM NaCl, 20 mM $MgCl_2$, 2 mM ATP, 10 mM DTT, and purified CBP−McbBCD synthetase (∼0.08 mg/mL) in a total volume of 100 μL. Assays were incubated at 37 °C for 24 h. The MBP tag was cleaved with thrombin (0.25 unit, 25 °C, 2 h), immediately frozen, and stored at −20 °C until HPLC purification.

Each cleaved McbA$_{1-46}$ fragment was purified by analytical C_{18} reversed-phase HPLC (solvent A = water/0.1% TFA; solvent B = acetonitrile/0.1% TFA; 32−45% linear gradient of B over 13 min, 1.5 mL/min; t_R ∼ 8 min). A UV−Vis diode array detector was utilized to obtain chromatograms at 220, 254, and 280 nm. Lyophilized peptide was redissolved in 30 μL of freshly prepared 10 mM DTT in 1:1 water/acetonitrile, and submitted for MALDI-MS analysis.

Table 2: MBP−McbA$_{1-46}$ Substrate Analogues and Selection Sites Used in Their Construction

analogue	plasmid	method	absent sites
GSC (wt)	pMSS10	USE	*Sma*I
GSC (wt)	pMSS11	PCR	−
GTCG	pMSS12	PCR	*Sma*I
GSCN	pMSS14	USE	*Sma*I, *Cla*I
GSTG	pMSS16	USE	*Sma*I
ASCG	pMSS23	USE	*Sma*I, *Cla*I
DSCG	pMSS24	USE	*Sma*I, *Cla*I
KSCG	pMSS25	USE	*Sma*I, *Cla*I
G_{11}SC	pMSS26	PCR	*Sma*I
G_9SC	pMSS27	PCR	*Sma*I
G_7SC	pMSS28	PCR	*Sma*I
G_5SC	pMSS29	PCR	*Sma*I
G_3SC	pMSS30	PCR	*Sma*I
GSCA	pMSS31	USE	*Sma*I, *Cla*I
GSCD	pMSS32	USE	*Sma*I, *Cla*I
GSCH	pMSS33	USE	*Sma*I, *Cla*I
GSCV	pMSS34	USE	*Sma*I, *Cla*I

RESULTS

Construction of Deletions and Point Mutations in the McbA$_{1-46}$ Sequence and Purification of Fusion Proteins To Test as Substrates. To facilitate both substrate purification and generation of substantial quantities of material, we expressed all the mutant McbA fragments as fusion proteins downstream of, and in-frame with maltose-binding protein (MBP−McbA$_{1-46}$). The MBP−McbA fusions incorporate a thrombin restriction site allowing for proteolytic removal of the MBP domain after treatment with microcin synthetase, and subsequent mass spectrometry analysis of heterocycle content in various McbA$_{1-46}$ mutant sequences. Typically, for the substrates listed in Table 2, 10 mg of the 47-kDa fusion protein was obtained in > 90% purity by one-step amylose affinity column purification from a 250 mL culture.

Affinity Purification of Microcin Synthetase Tagged with a Calmodulin-Binding Peptide at the N Terminus of McbB. To facilitate the isolation of synthetase, an affinity strategy was utilized by inserting the 26 residue calmodulin-binding peptide at the N terminus of McbB. It was presumed that this modification of McbB would not disrupt interaction with the McbC and McbD subunits and would allow for a single-step purification by adsorption of the CBP−McbB, McbC, and McbD microcin synthetase complex on a calmodulin-agarose column in the presence of Ca^{2+} followed by specific elution with EGTA (*23*, *25*). In the event, enzymatic activity corresponding to the desired CBP-tagged microcin synthetase was detected in crude extracts adsorbed on the affinity column and could be eluted in active form, although the elution conditions needed to be stringently controlled. An initial elution in the presence of 150 mM NaCl, 2 mM EGTA (elution 1) afforded synthetase that copurified with a 53 kDa contaminant (Figure 4). Pure synthetase was subsequently eluted by lowering the ionic strength of the buffer. However, the enzymatic activity in these dilute "low salt" fractions was rapidly lost upon storage, and efforts to concentrate the synthetase by ultrafiltration led to loss of protein due to nonspecific adsorption. Various protocols were therefore screened for the second elution step, and elution with 2 mM EGTA in the presence of 300 mM NaCl and a nonionic detergent (0.1% Triton-X100) was found to stabilize the isolated synthetase complex. The purity of these "high salt" fractions (elution 2) was excellent as illustrated in Figure 4.

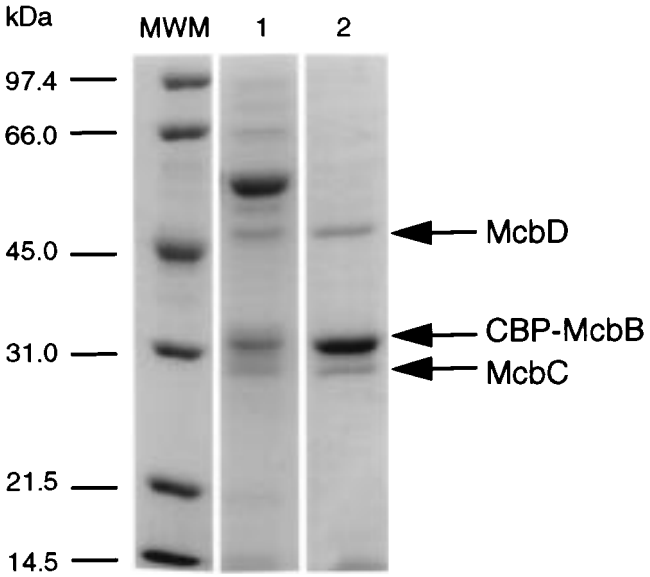

FIGURE 4: Overproduction and purification of CBP-tagged MccB17 synthetase complex. MWM, molecular mass markers; lane 1, first elution of the synthetase complex from the calmodulin affinity column with EGTA, as decribed under Experimental Procedures; lane 2, second elution of the CBP-tagged synthetase from the affinity column with EGTA and Triton X-100. The synthetase preparation is enriched in CBP-tagged McbB, which is the direct target of the calmodulin affinity resin.

Only the three CBP−McbB, McbC, and McbD subunits were detected. The extra 3.6 kDa provided by the CBP domain in the CBP−McbB fusion allows resolution of CBP−McbB and McbC in SDS gels whereas in wild-type complex McbB (32.7 kDa) and McbC (30.8 kDa) migrate together. The kinetic parameters for the CBP-tagged microcin synthetase complex with MBP−McbA$_{1-46}$ as substrate were $K_M = 0.6$ μM; $k_{cat} \sim 0.3$ min^{-1}, comparable to $K_M = 2.3$ μM, $k_{cat} \sim 0.2$ min^{-1} for the native complex with synthetic McbA$_{1-46}$ as substrate (*12*).

Distance Dependence for the Polyglycine Linker between the Propeptide Recognition Element and the First Residue Cyclized in MBP−McbA Fusion Protein Substrates. During maturation of prepromicrocin B17 to microcin B17, the 26 aa propeptide is proteolytically removed, but only after synthetase-mediated conversion of downstream Ser and Cys residues to heterocycles; the mature microcin antibiotic encompasses residues 27−69 of its precursor, with the first downstream heterocycles comprising the fused 4,2-oxazole−thiazole derived from the tripeptide moiety Gly^{39}−Ser^{40}-Cys^{41} (*5*). Of the intervening 13 residues between the end of the propeptide and Ser^{40}, 11 are glycine, suggesting that this linker region is likely to be highly flexible and unstructured. Since the specificity-conferring region of substrate McbA had to be *in cis*, covalently connected to residues 27−69, we addressed the issue of distance dependence between the 26 residue propeptide and the first cyclized serine residue by constructing a set of glycine deletion mutants in the MBP−McbA$_{1-46}$ substrate framework. Posttranslational modification activity of the microcin synthetase complex was assessed in a previously described Western assay (*12*) with antibody specific for heterocycle detection. Figure 5A shows data at 2 h time points for MBP−McbA$_{1-46}$ ("wild type"), containing 10 glycines in the polyglycine linker (residues 30−39, numbering scheme identical to that of prepromicrocin

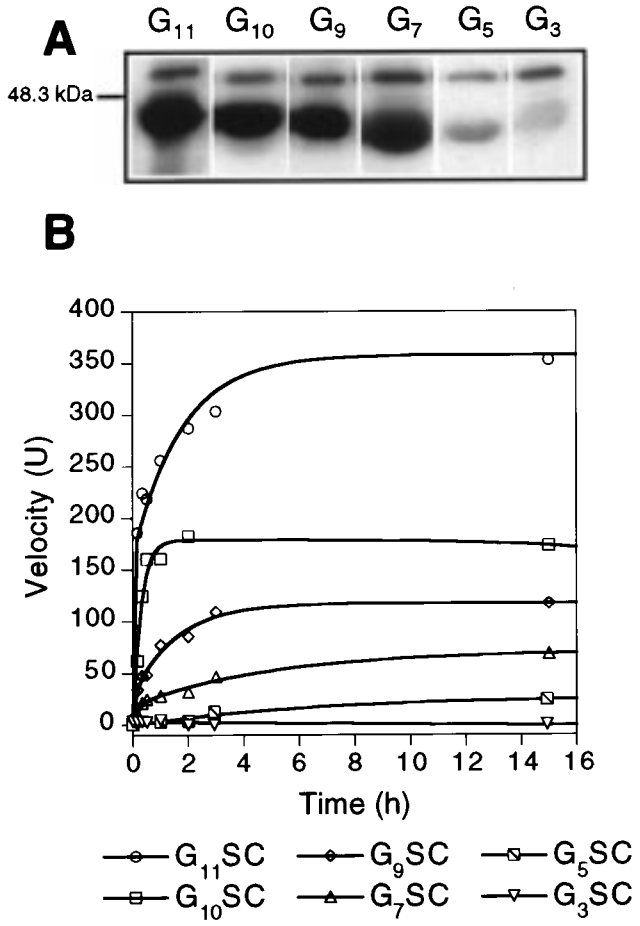

FIGURE 5: Protein immunoblot analysis of the MBP−McbA$_{1-46}$ glycine deletion/insertion mutants. (A) Protein immunoblots of 2 h incubations of substrate analogues with synthetase, probed sequentially with polyclonal rabbit anti-MccB17 and goat anti-rabbit antibodies as described under Experimental Procedures. The number of contiguous glycines in the linker of each construct [G$_n$SC, n = 11, 10 (wt), 9, 7, 5, 3] is depicted for each lane. Product formation drastically decreases for linkers incorporating less than seven glycines. The ~67 kDa band in each lane arises from nonspecific recognition of a contaminant in the synthetase preparation by the polyclonal antibodies. (B) Kinetic analysis of product formation in the above constructs obtained from Western assays. Data are normalized to internal or external standards as described under Experimental Procedures.

B17), labeled G$_{10}$. Also shown are data for various deletions of 1 (G$_9$), 3 (G$_7$), 5 (G$_5$), and 7 (G$_3$) of the 10 glycines in the linker region, along with results for the insertion of 1 extra glycine (G$_{11}$). Qualitatively, it is clear that the G$_{11}$SC, G$_9$SC, and G$_7$SC MBP−McbA$_{1-46}$ analogues are substrates, while the G$_5$SC and G$_3$SC analogues are marginal at best. To further compare the deletion series, initial velocity studies were conducted, keeping each substrate concentration at 20 μM (estimated to be ~20K_M for the G$_{10}$SC wild-type MBP−McbA$_{1-46}$ sequence). Figure 5B shows the comparative rate data over a 15 h time period of incubation. An extrapolation of rates reveals that the elongation of the polyglycine linker by one residue (G$_{11}$SC) is accompanied by a 2-fold increase in the initial rate compared to that of wild type (G$_{10}$SC). In turn, G$_9$SC is approximately 5-fold slower than G$_{10}$SC and G$_7$SC is 13-fold slower still. Turnover of G$_5$SC is barely above background, and that of G$_3$SC is at background, revealing a distance dependence and a minimal length of the glycine linker region between the propeptide recognition site and the site of posttranslational cyclization. Mass spectroscopic analyses of assay mixtures supported these observations. Thus, while monocyclic intermediates and bicyclic products were readily observed by mass spectrometry for incubations of G$_n$SC (n = 11, 10, 9), and, to a lesser extent, for assays of G$_7$SC with synthetase, no heterocyclic species were detected in the G$_3$SC assay (Table 3).

Table 3: MALDI-MS Data for the Detection of Uncyclized McbA$_{1-46}$ Peptides, Monocyclic Intermediates, and Bisheterocyclic Products[a]

McbA$_{1-46}$ analogue	uncyclized peptide [MH]$^+$ calcd	uncyclized peptide [MH]$^+$ obsd	monocyclic species [(M−20)H]$^+$ obsd	bisheterocyclic product [(M−40)H]$^+$ obsd
G$_{11}$SC	4364	4364	+	+
G$_{10}$SC (wt)	4307	4302	+	+
G$_9$SC	4250	4253	+	+
G$_7$SC	4136	4138	+	−
G$_3$SC	3907	3909	−	−
ASCG	4321	4321	−	−
DSCG	4365	4367	−	−
KSCG	4378	4376	−	−
GSCA	4321	4325	+	+
GSCD	4365	4365	−	−
GSCN	4364	4366	+	−
GSCV	4349	4351	+	−
GSTG	4305	4305	−	−
GTCG	4321	4322	−	−

[a] Each McbA$_{1-46}$ peptide incorporates Gly-Ser at the N-terminus following thrombin cleavage of the parent MBP fusion protein. A synthetic polypeptide (corresponding to the G$_2$SC analogue of McbA$_{1-46}$, M = 3705 amu) was used as the internal calibration standard.

To determine whether the failure of microcin B17 synthetase to process the G$_3$SC deletion construct was indeed not failure to bind substrate through the 1−26 propeptide recognition element but rather an inability to simultaneously recognize propeptide and position the GSC element of substrate at the enzyme active site, an inhibition study of G$_{10}$SC processing by the G$_3$SC MBP−McbA$_{1-46}$ fusion protein was conducted. Panel A of Figure 6 indicates that the G$_{10}$SC MBP−McbA$_{1-46}$ fusion exhibits well-behaved Michaelis−Menten kinetics in the Western assay. Panel B shows data in which inclusion of G$_3$SC at 0.3, 1, or 2 μM levels and varying concentrations of G$_{10}$SC leads to demonstrable inhibition, with a pattern that is consistent with a mixed noncompetitive scheme (*26*). To the extent that it might be mixed noncompetitive inhibition, kinetic constants can be deconvoluted as shown in Figure 7, where the K_s of 1.9 μM is comparable to the G$_{10}$SC K_M of 0.6 μM (panel A) and K_{IS} = 0.9 μM; K_{II} = 1.7 μM. Given that the K_I values of G$_3$SC are in the low micromolar range and approximate the K_M of wild-type substrate, it is likely that the failure of G$_5$SC and G$_3$SC deletion mutants to get processed to heterocyclic products is due to a k_{cat} rather than a K_D effect.

Sequence Selectivity for the GSCG Motif in Heterocycle Formation by Microcin Synthetase. The first question asked in this probe of specificity was whether threonine could replace serine or cysteine as the only other of the 20 amino acids found in proteins with a nucleophilic β substituent capable of cyclization. The GSTG and GTCG mutants of MBP−McbA$_{1-46}$ were inactive in the Western assay to detect heterocycle formation (data not shown). Since it was not clear whether the polyclonal antibody detection reagent

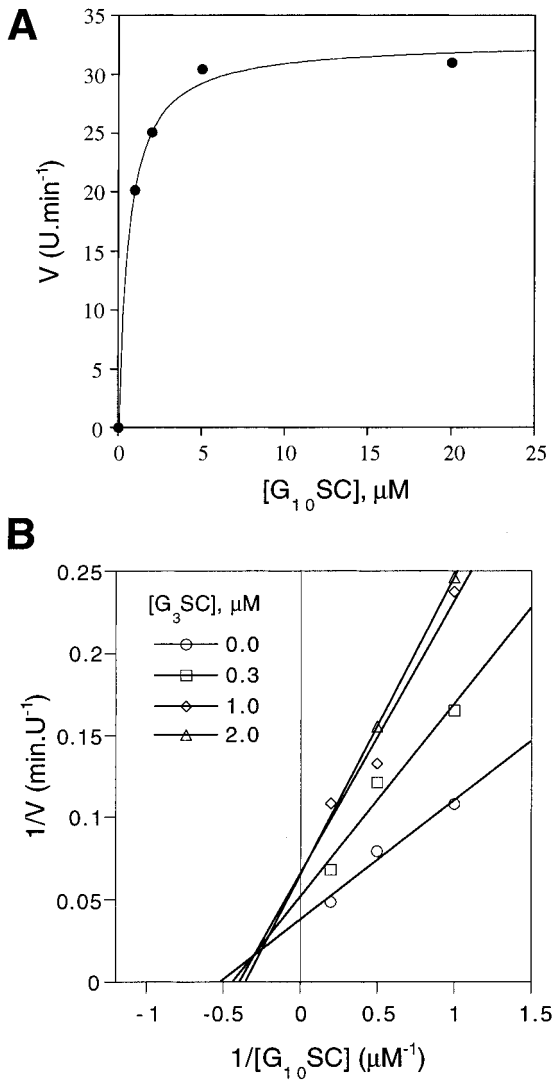

FIGURE 6: Evaluation of kinetic parameters for the MBP−$McbA_{1-46}$ substrate. (A) Michaelis−Menten plot for turnover of MBP−$McbA_{1-46}$ by CBP−McbBCD. Velocities (V) were obtained by Western assays ($K_M = 0.6\ \mu M$; $k_{cat} \sim 0.3\ min^{-1}$). (B) Double-reciprocal (Lineweaver−Burk) plots for inhibition of $G_{10}SC$ turnover by G_3SC. The pattern is consistent with mixed noncompetitive inhibition.

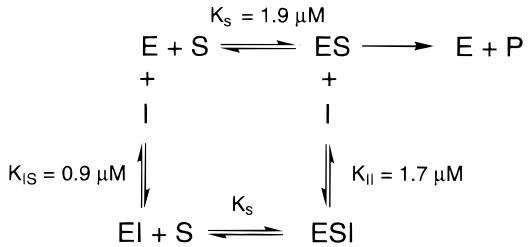

FIGURE 7: Mixed noncompetitive inhibition of MBP−$McbA_{1-46}$ (S) by substrate analogue G_3SC (I), and the equilibrium constants for such a scheme evaluated from the plots depicted in Figure 6.

would in fact recognize a β-methyloxazole in place of an oxazole either singly or in oxazole−thiazole combinations, the incubations were analyzed by mass spectrometry for heterocycle content as noted in the next section. No cyclized product was detected (Table 3), in agreement with the data from the Western assay.

Next, the selectivity for -XSCG- and -GSCX- was probed to analyze tolerance for residues other than glycine just

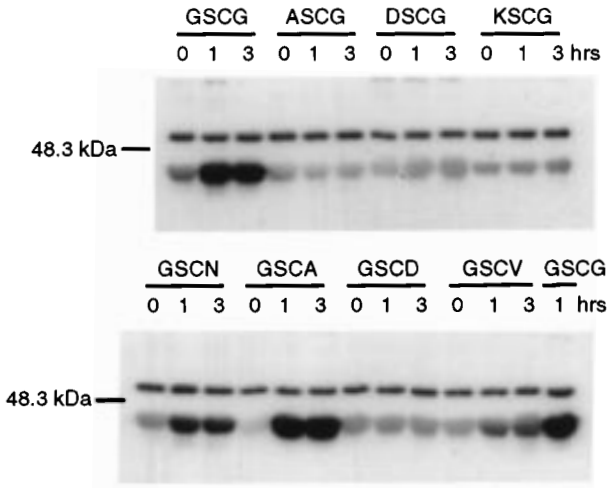

FIGURE 8: Protein immunoblots for incubations of the GSCX and XSCG MBP−$McbA_{1-46}$ substrate analogues with MccB17 synthetase. Time-dependent product formation is evident for the GSCG (wt), GSCN, GSCA, and GSCV constructs. The ~67 kDa band in each lane arises from nonspecific recognition of a contaminant in the synthetase preparation by the polyclonal antibodies used in the Western assay.

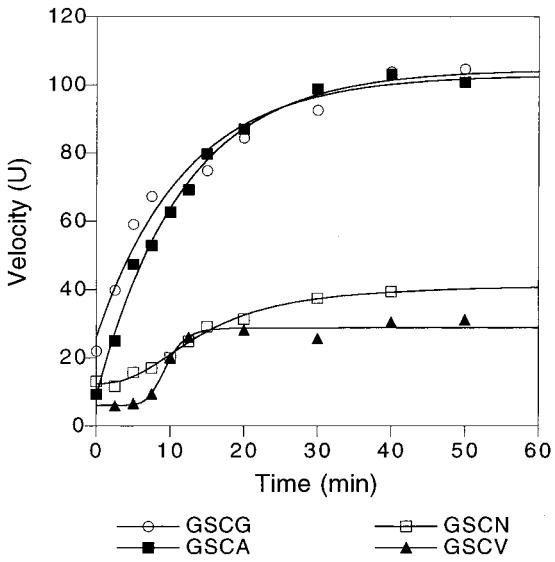

FIGURE 9: Kinetics of heterocyclization for the GSCG, GSCA, GSCN, and GSCV MBP−$McbA_{1-46}$ substrate analogues. Reaction velocities were obtained by Western assays and are normalized as described under Experimental Procedures.

preceding and following the serine and cysteine processing sites in microcin B17. As shown in Figure 8 for XSCG mutants, when Gly^{39} was replaced with aspartate, or lysine, these charged residues were not tolerated. Even the most conservative natural amino acid substitution, Gly^{39}→Ala in mutant ASCG, led to no product that could be detected by either antibody or mass spectrometry. It therefore appears that glycine is essential in Gly-Ser and Gly-Ser-Cys sequences (and most likely at Gly-Cys sites as well). When the GSCX MBP−$McbA_{1-46}$ mutants were constructed, purified, and analyzed (Figure 8), the GSCD protein failed to serve as substrate while initial rate data (Figure 9) indicate GSCA(~GSCG) ≫ GSCN, GSCV, all with signals above background, suggesting that the downstream residue (X) in the -GSCX- sequence is less restrictive in the enzymatic heterocyclization chemistry under examination. As a control experiment, the inhibition of MBP−$McbA_{1-46}$ turnover upon

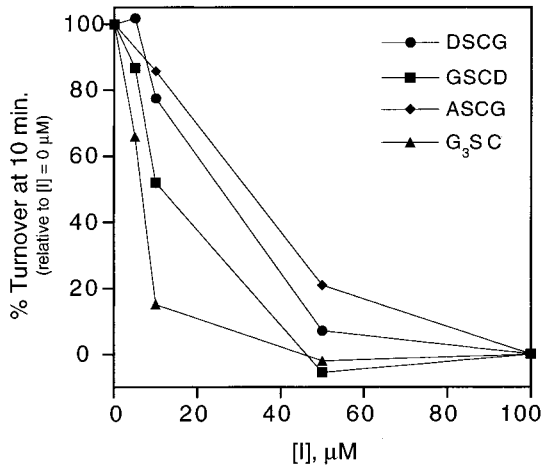

FIGURE 10: Inhibition of substrate (MBP−$McbA_{1-46}$, GSC) turnover upon titration with DSCG, ASCG, or G_3SC substrate analogues, measured by Western assay after a 10 min incubation with synthetase.

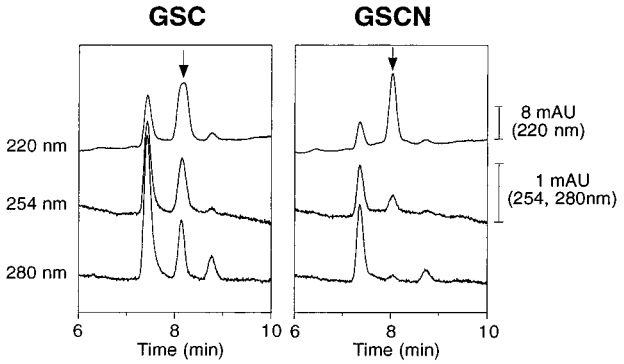

FIGURE 11: HPLC chromatograms of synthetase-processed and thrombin-cleaved $McbA_{1-46}$ fragments for the GSC ("wild type") and GSCN substrates. In each case, chromatograms were obtained simultaneously at 220, 254, and 280 nm. The retention time of $McbA_{1-46}$ polypeptides is invariant with respect to heterocycle content under these conditions (t_R ~8 min, $McbA_{1-46}$ peaks denoted by arrows). Mono- and bisheterocyclization in GSC is accompanied by significant absorbances at 254 and 280 nm, respectively, whereas the slow turnover of GSCN results in only a slight absorbance at 254 nm, consistent with the formation of a single oxazole/thiazole. For the various substrate analogues investigated, fractions corresponding to the above peaks were submitted for MALDI-MS analysis and provided the data listed in Table 3.

titration with DSCG, GSCD, or ASCG was also evaluated by Western blots to determine whether the XSCG and GSCX mutants were competent with regard to recognition by the synthetase. The results of the inhibition assays (at a substrate concentration of 7 μM) are presented in Figure 10. The IC_{50} values for all the substrate analogues investigated were in the 11−33 μM range, comparable to that of G_3SC (7 μM). Thus, perturbation of the residues immediately upstream and downstream of the heterocycle sites does not appreciably affect initial recognition by the synthetase.

Incubations of select substrate analogues with synthetase were further analyzed by mass spectrometry to confirm that absence of product formation (as indicated by Western blots) was not due to an inability of the anti-MccB17 antibody to recognize altered -GSCX- and -XSCG- heterocyclic epitopes. For the GSCN and GSCV substrate analogues, only monocyclic ($[MH]^+-20$) intermediates were observed by mass spectrometry. This result may be due to an inability to detect by mass spectrometry the low levels of bicyclic product obtained in the slow turnovers of these substrate analogues. Alternatively, only a single Ser/Cys in the -GSCX- sequence might be preferentially cyclized when the downstream residue is Asn or Val. A comparison of chromatograms acquired at different wavelengths during the HPLC purification of synthetase-processed $McbA_{1-46}$ fragments supports the second hypothesis. Thus, a significant absorbance at 254 nm (due to individual oxazole and thiazole moieties) and at 280 nm due to the 4,2-fused bisheterocycle (*8*) is observed for the thrombin-proteolyzed $McbA_{1-46}$ fragment obtained after processing of the GSC substrate by the synthetase (Figure 11). In contrast, only a small absorbance at 254 nm is observed for the GSCN analogue, which together with a negligible absorption at 280 nm is consistent with the slow formation of a single heterocycle. The UV spectroscopy and mass spectrometry data (Table 3) were also consistent with the Western analysis for the other substrate analogues examined, which confirmed that the Western assay could be used as a diagnostic tool to probe heterocycle formation even for non-native McbA substrate analogues.

DISCUSSION

The DNA gyrase inhibitor microcin B17 belongs to a growing family of pharmaceutically important compounds of peptidic origin that incorporate thiazoles, oxazoles, and the corresponding 4,5-dihydroheterocycles. However, the biological significance of these structures has only recently been demonstrated in diverse processes ranging from DNA intercalation in the antitumor drug bleomycin (*27*) to metal coordination in the siderophore yersiniabactin (*28*). It is possible that the significant changes in geometry, which accompany heterocycle formation, may also improve the stability of these compounds *in vivo*, especially for polypeptides such as microcin B17. An evaluation of the selectivity and catalytic properties of the synthetase that mediates heterocycle biosynthesis in MccB17 is therefore a prelude to the rational chemoenzymatic development of new compounds with potential novel antitumor, antiviral, and antifungal properties.

Although microcin B17 synthetase is known to be composed of three proteins (McbB, -C, and -D) that couple ATP hydrolysis to heterocycle formation in McbA, the stoichiometry and function of each individual subunit and the mode of ATP cleavage have yet to be determined. We have previously reported a four-column chromatographic purification of the microcin synthetase complex from *E. coli* (*12*) that takes approximately 1 week and affords the purified complex in low yield with modest specific activity. To facilitate enzymatic characterization, a convenient purification of the multisubunit enzyme complex is presented. CBP-tagged McbB allows purification of milligram quantities of the synthetase complex (CBP−McbBCD) in a single affinity chromatography step and enables *in vitro* analyses of heterocycle formation by Western blot, UV−Vis, and mass spectroscopies. The affinity-purified CBP−microcin synthetase is free of any detectable HtpG protein, the chaperone that accompanies microcin synthetase when purified from *E. coli*. Furthermore, the kinetic properties of CBP-tagged synthetase seem comparable to the nontagged complex, although the abundance of McbC and McbD subunits is lower than that of the tagged McbB protein, which is the direct target of the affinity resin. This enrichment in McbB

could be a limitation for some analyses such as stoichiometry evaluation of the three McbB, -C, and -D subunits in active complexes. One property that seemed altered between native microcin synthetase and CBP-tagged enzyme was the increased tendency of the latter to undergo a loss of activity both in subsequent manipulations and upon storage. However, the tagged complex could be stored at −80 °C for months at concentrations >0.1 mg/mL without significant loss of activity, and was therefore useful as a source of synthetase for the studies reported herein.

A second issue regarding the investigation of MccB17 synthetase concerned the construction of alternate substrates. Previous studies have established that the key recognition element is the propeptide sequence ($McbA_{1-26}$) (*12*, *13*), which is proteolytically removed after posttranslational modification of downstream Ser and Cys residues (*5*). This phenomenon is reminiscent of the posttranslational carboxylation of glutamyl residues in blood coagulation proteins by the vitamin K-dependent γ-glutamyl carboxylase (*29*), which targets an analogous amphipathic helical "γ-carboxylation recognition site" (γ-CRS) just upstream of the run of residues to be processively modified (*30*). However, unlike the γ-CRS, which can function *in trans* (*31*), posttranslational processing of preproMccB17 by the synthetase to date requires covalent attachment of the leader propeptide. Hence, substrate analogues have to be at least 41 residues in length, since the first (bisheterocyclic) cyclization site is located 14 residues downstream of the leader ($Gly^{39}Ser^{40}$-Cys^{41}). We have focused on $McbA_{1-46}$ fragments to test downstream sequence requirements. Recombinant protein expression was used as a cost-effective alternate to chemical peptide synthesis for the generation of substrate analogues. Specifically, the fusion of MBP to $McbA_{1-46}$ has enabled a one-step purification for 15 mutant substrates in multimilligram quantities. In this regard, it has been shown that MBP−$McbA_{1-69}$ is a substrate for heterocycle formation (Madison and Kolter, unpublished experiments) as assessed by a Western assay with a polyclonal antibody that recognizes proMccB17 and mature microcin B17 (Figure 1), but not preproMccB17 (*5*). The $McbA_{1-46}$ fragment was appropriate for analysis since it encompassed the first bisheterocyclic site, which is known to be completely processed by the synthetase *in vitro* (*12*).

Distance Dependence of the Polyglycine Linker between Propeptide and the First Cyclization Site. The conformational flexibility of glycine implies that the -Val^{27}-Gly-Ile-$[Gly]_{10}$- linker, which connects the McbA propeptide to downstream processing sites, is considerably disordered. Nevertheless, this sequence functions as a spacer, and apparently positions the -Gly^{39}-Ser^{40}-Cys^{41}- sequence in correct register with the synthetase active site at a defined distance from the site of propeptide recognition. A significant decrease in substrate turnover for linkers shorter than 10 residues (e.g., G_7SC) suggests that the synthetase active site is located 16−30 Å distant from the propeptide recognition domain. These estimates correspond to the rms separation of terminii in a 10 residue random coil peptide (*32*), and to the distance spanned by a β-strand of the same length, respectively. The prerequisite for a correct alignment between propeptide, residues to be processed, and the synthetase active site is consistent with directional modification of the McbA substrate downstream from the propeptide.

Scheme 1

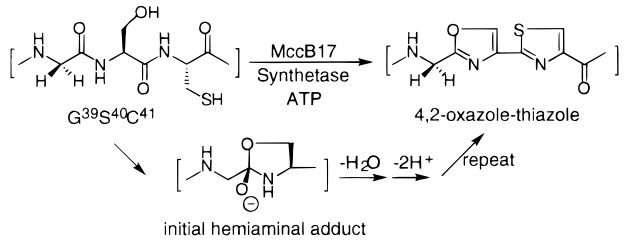

It also raises the possibility of kinetic processivity, perhaps with heterocycle formation resulting in an increased affinity or positive cooperativity for subsequent unprocessed sites.

Incompatibility of Thr as a Substrate. Both Western analysis and mass spectrometry confirmed that heterocycle formation does not occur in the GSTG and GTCG substrate analogues. Thus, a threonine substitution in either the first or the second position of the SC pair blocks formation of *both* the mono and the bis heterocycle. Apparently, the steric consequences of a β-methyl substituent serve to block one or more steps in heterocycle formation (cyclization, dehydration, and desaturation) or combinations thereof. No β-methyloxazoline product ($[MH]^+-18$) or oxazole ($[MH]^+-20$) was detected by mass spectrometry, although the stability of such a species to the conditions of MALDI-MS has not been evaluated since appropriate standards are not available. Given the existence of β-methyloxazolines and β-methyloxazoles in other peptide-based natural products [e.g., thiangazole (*33*), tantazole (*34*)], the inability to process Thr points either to a different mechanism of biosynthesis for the latter, or more likely to a more restrictive steric tolerance in MccB17 synthetase. In either case, it is unlikely that MccB17 synthetase will yield β-methyloxazole-containing antibiotic products

Significance of Glycine as the Upstream Residue. Mutational analysis of Gly^{39} revealed that this residue is critical for heterocyclization. The carbonyl group of this glycine (and all other glycines in -Gly-Ser- and -Gly-Cys- sequences that get cyclized) is incorporated into the nascent oxazoline or thiazoline ring that is formed (Scheme 1).

The lack of an α-substituent and/or the unique conformational flexibility of glycine is essential for side chain-to-backbone cyclization of ensuing residues in -Gly-Ser-Cys-, and presumably at the other -Gly-Cys-Ser-, -Gly-Ser-, and -Gly-Cys- sequences cyclized by MccB17 synthetase. The lack of steric hindrance at the upstream residue together with deformation of the appropriate amide bond from the planar resonance-stabilized form may be required for the synthetase to initiate cyclization in a low-energy barrier mode, to form the initial cyclic hemiaminal adduct. The prerequisite for glycine at the upstream site may be a specificity feature of MccB17 synthetase but not a strict mechanistic requirement for peptide/amide conversions to thiazolines and oxazolines. For example, an -Ile-Cys- sequence is converted to the corresponding 2-alkylthiazoline by the nonribosomal peptide synthetase bacitracin synthase (*35*). In some analogy, 2-hydroxybenzoyl-Cys/Ser/Thr sequences are processed to 2-hydroxyphenyl-thiazolines/oxazolines/β-methyloxazolines during the biosynthesis of yersiniabactin (*28*), exochelins (*36*), and parabactin (*37*), respectively. On the other hand, this difference in selectivity for the acyl partner in the amide bond attacked by Ser, Cys, or Thr nucleophilic side

chains might reflect a distinct mechanism of heterocycle formation in these enzyme-bound thiol−template nonribosomal peptide synthetases, compared to the posttranslational modification activity of MccB17 synthetase.

Evaluation of the Downstream Residue in the -GSCG- Sequence. An increased tolerance for mutations at the glycine downstream of processed Ser/Cys sites is consistent with a limited sensitivity of heterocyclization to this position, implying that the downstream residue serves more of a "bystander role" and is much less intimately involved than the upstream glycine in the mechanism of cyclization. Nevertheless, charged or polar residues are not tolerated at this position, and most likely influence the regioselectivity of heterocycle biosynthesis in microcin B17. Two serine residues (Ser^{52}, Ser^{67}) remain unprocessed in the mature antibiotic (Figure 1B), and are upstream of asparagine and histidine, respectively. While we could speculate about decreased cyclization efficiency toward the C-terminus of the 69 aa prepromicrocin B17, Ser^{52} is bypassed while further downstream, Ser^{56}, Ser^{62}, and Ser^{65} are cyclized. In fact, although both Ser^{52} and Ser^{56} are embedded in -Gly-Cys-Ser- triads just two residues apart of each other, only the latter is fully processed to the bisheterocycle. It is probable that Asn^{53} in the -Gly^{50}-Ser-Cys-Asn- sequence and His^{68} in the -Gly^{66}-Ser-His- sequence are acting as stop signals for heterocyclization of the upstream Ser. Thus, when Asn and His were placed downstream of the bisheterocyclization site at -Gly^{39}-Ser^{40}-Cys^{41}- in mutants GSCN and GSCH, respectively, very slow rates of cyclization were observed by Western blots for the former, and no turnover was detected in the latter (data not shown). Furthermore, no bisheterocyclic product could be detected by UV and mass spectroscopies for incubations of GSCN with synthetase. As we have observed a very good correlation of Western assay and UV/MS data for single and bisheterocycle formation (Belshaw et al., unpublished experiments), it appears that Asn and His seriously disrupt processing by MccB17 synthetase.

The studies described herein begin to delineate the sequence context of serines and cysteines, which dictates the kinetics and efficiency of cyclization of the McbA substrate by MccB17 synthetase. Residues upstream (absolute requirement for glycine) and downstream of serine and cysteine exert steric and electronic effects that can affect formation of one or both thiazole and oxazole heterocycles (in single or tandem 4,2-fused systems). The requirements for a propeptide (residues 1−26) and a flexible polyglycine spacer of a minimal length define a distance dependence between the initial high-affinity recognition site (for propeptide) and the first cyclizable residue. Therefore, the polyglycine linker serves a spacer function to position -Gly-Ser-Cys-, -Gly-Cys-Ser-, -Gly-Cys-, and -Gly-Ser- moieties in the catalytic site, suggesting the model depicted in Figure 12 for substrate recognition by the synthetase. Although the exact roles played by each McbB, -C, and -D subunit in the process are not yet known, we envisage initial recognition of the *cis*-acting propeptide by the synthetase, followed by alignment of the first (bisheterocyclization) sequence with the enzyme active site by the flexible polyglycine spacer. The latter requires at least five glycine residues for observable turnover of substrate. Cyclization of cysteines and serines subsequently occurs in an as yet to be determined processive or distributive manner, with the conformational flexibility of the upstream glycines being critical for heterocycle formation. Polar residues (Asn, His) positioned downstream of cyclizable serines or cysteines disrupt processing by the synthetase and may dictate the regioselectivity of heterocycle formation. This model, together with complementary analyses of regioselectivity and kinetics of single-ring and fused bisheterocycle variants (Belshaw et al., manuscript in preparation), should help to create a knowledge base for planning combinatorial biosynthetic strategies for microcin B17 analogues with altered antibacterial properties.

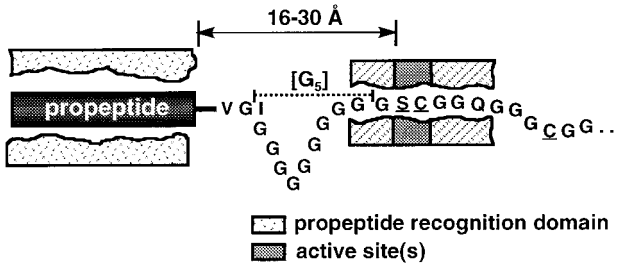

FIGURE 12: Proposed model for the recognition of McbA substrate by microcin B17 synthetase discussed in the text. Propeptide recognition in cis serves to align cyclizable residues (underlined) with the synthetase active site. A polyglycine tether of at least five glycines is required in the above process. See text for details.

ACKNOWLEDGMENT

We are grateful to Ms. Michelle Obenauer of the Howard Hughes Biopolymer facility for MALDI-MS analyses and to Dr. Charles Dahl of the Biopolymers Laboratory at Harvard Medical School for DNA sequencing. We thank Dr. Jill Milne for helpful and insightful discussions, and for critical reading of the manuscript.

REFERENCES

1. Kolter, R., and Moreno, F. (1992) *Annu. Rev. Microbiol.*, 141−163.
2. San Millán, J. L., Kolter, R., and Moreno, F. (1985) *J. Bacteriol. 163*, 1016−1020.
3. San Millán, J. L., Kolter, R., and Moreno, F. (1985) *J. Bacteriol. 163*, 275−281.
4. Davagnino, J., Herrero, M., Furlong, D., Moreno, F., and Kolter, R. (1986) *Proteins: Struct., Funct., Genet. 1*, 230−238.
5. Yorgey, P., Davagnino, J., and Kolter, R. (1993) *Mol. Microbiol. 9*, 897−905.
6. Bayer, A., Freund, S., Nicholson, G., and Jung, G. (1993) *Angew. Chem., Int. Ed. Engl. 32*, 1336−1339.
7. Yorgey, P., Lee, J., Kordel, J., Vivas, E., Warner, P., Jebaratnam, D., and Kolter, R. (1994) *Proc. Natl. Acad. Sci. U.S.A. 91*, 4519−4523.
8. Bayer, A., Freund, S., and Jung, G. (1995) *Eur. J. Biochem. 234*, 414−426.
9. Garrido, M. C., Herrero, M., Kolter, R., and Moreno, F. (1988) *EMBO J. 7*, 1853−1862.
10. Vizán, J. L., Hernández-Chico, C., del Castillo, I., and Moreno, F. (1991) *EMBO J. 10*, 467−476.
11. Liu, L. F. (1989) *Annu. Rev. Biochem. 58*, 351−375.
12. Li, Y.-M., Milne, J. C., Madison, L. L., Kolter, R., and Walsh, C. T. (1996) *Science 274*, 1188−1193.
13. Madison, L. L., Vivas, I. E., Li, Y.-M., Walsh, C. T., and Kolter, R. (1997) *Mol. Microbiol. 23*, 161−168.
14. McCafferty, D. G., Lessard, I. A. D., and Walsh, C. T. (1997) *Biochemistry 36*, 10498−10505.
15. Sambrook, J., Fritsch, E. F., and Maniatis, T. (1989) *Molecular Cloning: A Laboratory Manual*, 2nd ed., Cold Spring Harbor Laboratory, Cold Spring Harbor, NY.

16. Saiki, R. K., Gelfand, D. H., Stoffel, S., Scharf, S. J., Higuchi, R., Horn, G. T., Mullis, K. B., and Erlich, H. A. (1988) *Science 239*, 487−491.
17. Guan, C., Li, P., Riggs, P. D., and Inouye, H. (1988) *Gene 67*, 21−30.
18. Deng, W. P., and Nickoloff, J. A. (1992) *Anal. Biochem. 200*, 81−88.
19. Edelhoch, H. (1967) *Biochemistry 6*, 1948−1954.
20. Pace, C. N., Vajdos, F., Fee, L., Grimsley, G., and Gray, T. (1995) *Protein Sci. 4*, 2411−2423.
21. Blumenthal, D. K., Takio, K., Edelman, A. M., Charbonneau, H., Titani, K., Walsh, K. A., and Krebs, E. G. (1985) *Proc. Natl. Acad. Sci. U.S.A. 82*, 3187−3191.
22. Takio, K., Blumenthal, D. K., Walsh, K. A., Titani, K., and Krebs, E. G. (1986) *Biochemistry 25*, 8049−8057.
23. Zheng, C.-F., Simcox, T., Xu, L., and Vaillancourt, P. (1997) *Gene 186*, 55−60.
24. Harlow, E., and Lane, D. (1988) *Antibodies: A Laboratory Manual*, Cold Spring Harbor Laboratory, Cold Spring Harbor, NY.
25. Stofko-Hahn, R. E., Carr, D. W., and Scott, J. D. (1992) *FEBS Lett. 302*, 274−278.
26. Henderson, P. J. F. (1992) in *Enzyme Assays: A Practical Approach* (Eisenthal, R., & Danson, M. J., Eds.) pp 277−316, IRL Press, Oxford.
27. Kane, S. A., and Hecht, S. M. (1994) *Prog. Nucleic Acid Res. Mol. Biol. 49*, 313−352.
28. Drechsel, H., Stephan, H., Lotz, R., Haag, H., Zähner, H., Hantke, K., and Jung, G. (1995) *Liebigs Ann. Chem.*, 1727−1733.
29. Furie, B., and Furie, B. C. (1988) *Cell 53*, 505−518.
30. Hubbard, B. R., Jacobs, M., Ulrich, M. M. W., Walsh, C., Furie, B., and Furie, B. C. (1989) *J. Biol. Chem. 264*, 14145−14150.
31. Cheung, A., Engelke, J. A., Sanders, C., and Suttie, J. W. (1989) *Arch. Biochem. Biophys. 274*, 574−581.
32. Atkins, P. W. (1982) in *Physical Chemistry*, pp 835−842, Oxford University Press, Oxford.
33. Jansen, R., Kunze, B., Reichenbach, H., Jurkiewicz, E., Hunsmann, G., and Hofle, G. (1992) *Liebigs Ann. Chem.*, 357−359.
34. Carmeli, S., Paik, S., Moore, R. E., Patterson, G. M. L., and Yoshida, W. Y. (1993) *Tetrahedron Lett. 34*, 6681−6684.
35. Ishihara, H., and Shimura, K. (1988) *FEBS Lett. 226*, 319−323.
36. Wong, D. K., Gobin, J., Horwitz, M. A., and Gibson, B. W. (1996) *J. Bacteriol. 178*, 6394−6398.
37. Neilands, J. B. (1981) *Annu. Rev. Biochem. 50*, 715−731.

BI9728250